2017-06

Various effects of embedded intrapulse communications on pulsed radar

Hunt, Allison

Monterey, California: Naval Postgraduate School

NAVAL POSTGRADUATE SCHOOL

MONTEREY, CALIFORNIA

THESIS

VARIOUS EFFECTS OF EMBEDDED INTRAPULSE COMMUNICATIONS ON PULSED RADAR

by

Allison Hunt

June 2017

Thesis Co-Advisors: Ric A. Romero
Zachary Staples

THIS PAGE INTENTIONALLY LEFT BLANK

REPORT DOCUMENTATION PAGE

Form Approved OMB No. 0704–0188

1. AGENCY USE ONLY *(Leave Blank)*	2. REPORT DATE	3. REPORT TYPE AND DATES COVERED
	16 June 2017	Master's Thesis 07-01-2016 to 06-16-2017

4. TITLE AND SUBTITLE

VARIOUS EFFECTS OF EMBEDDED INTRAPULSE COMMUNICATIONS ON PULSED RADAR

5. FUNDING NUMBERS

6. AUTHOR(S)

Allison Hunt

7. PERFORMING ORGANIZATION NAME(S) AND ADDRESS(ES)

Naval Postgraduate School
Monterey, CA 93943

8. PERFORMING ORGANIZATION REPORT NUMBER

9. SPONSORING / MONITORING AGENCY NAME(S) AND ADDRESS(ES)

N/A

10. SPONSORING / MONITORING AGENCY REPORT NUMBER

11. SUPPLEMENTARY NOTES

The views expressed in this document are those of the author and do not reflect the official policy or position of the Department of Defense or the U.S. Government. IRB Protocol Number: N/A.

12a. DISTRIBUTION / AVAILABILITY STATEMENT

Approved for public release. Distribution is unlimited

12b. DISTRIBUTION CODE

13. ABSTRACT *(maximum 200 words)*

Despite the ubiquity of networked and radio frequency-emitting devices in the maritime domain, a robust understanding of the maritime cyber environment has not yet been fully developed. One particular area of interest within this larger environment is that of co-channel interference between radar and communications systems. The effects of a relatively low-power in-band communications interferer on a high-power radar are investigated. Software simulation is used to determine the probability of detection and power spectral density of the combined radar-communications signal for a pulsed radar. Additionally, the impact of an interfering communications signal on the range-Doppler map of a pulse Doppler radar is investigated. The perspective of a radar operator in a maritime environment is also considered. In all cases, the communications signal is parameterized by the radar-to-communications power ratio (RCR) and the symbol-rate-to-bandwidth ratio (SRBR). Finally, software simulation is validated for the probability of detection case by implementing the radar detector on a field-programmable gate array (FPGA) similar to what would be used in a radar receiver. In all cases, embedded communications are found to have relatively little effect on radar performance.

14. SUBJECT TERMS	15. NUMBER OF PAGES
Communications, radar, interference, probability of detection	61
	16. PRICE CODE

17. SECURITY CLASSIFICATION OF REPORT	18. SECURITY CLASSIFICATION OF THIS PAGE	19. SECURITY CLASSIFICATION OF ABSTRACT	20. LIMITATION OF ABSTRACT
Unclassified	Unclassified	Unclassified	UU

NSN 7540-01-280-5500

Standard Form 298 (Rev. 2–89)
Prescribed by ANSI Std. 239–18

THIS PAGE INTENTIONALLY LEFT BLANK

Approved for public release. Distribution is unlimited

VARIOUS EFFECTS OF EMBEDDED INTRAPULSE COMMUNICATIONS ON PULSED RADAR

Allison Hunt
Ensign, United States Navy
B.S.E.E, United States Naval Academy, 2016

Submitted in partial fulfillment of the
requirements for the degree of

MASTER OF SCIENCE IN ELECTRICAL ENGINEERING

from the

NAVAL POSTGRADUATE SCHOOL
June 2017

Approved by: Ric A. Romero
Thesis Co-Advisor

Zachary Staples
Thesis Co-Advisor

R. Clark Robertson
Chair, Department of Electrical and Computer Engineering

THIS PAGE INTENTIONALLY LEFT BLANK

ABSTRACT

Despite the ubiquity of networked and radio frequency-emitting devices in the maritime domain, a robust understanding of the maritime cyber environment has not yet been fully developed. One particular area of interest within this larger environment is that of co-channel interference between radar and communications systems. The effects of a relatively low-power in-band communications interferer on a high-power radar are investigated. Software simulation is used to determine the probability of detection and power spectral density of the combined radar-communications signal for a pulsed radar. Additionally, the impact of an interfering communications signal on the range-Doppler map of a pulse Doppler radar is investigated. The perspective of a radar operator in a maritime environment is also considered. In all cases, the communications signal is parameterized by the radar-to-communications power ratio (RCR) and the symbol-rate-to-bandwidth ratio (SRBR). Finally, software simulation is validated for the probability of detection case by implementing the radar detector on a field-programmable gate array (FPGA) similar to what would be used in a radar receiver. In all cases, embedded communications are found to have relatively little effect on radar performance.

THIS PAGE INTENTIONALLY LEFT BLANK

Table of Contents

List of Figures

List of Acronyms and Abbreviations

A/D	analog-to-digital
AIS	automatic identification system
AWGN	additive white Gaussian noise
BER	bit error ratio
BPSK	binary phase-shift keying
DPSK	differential phase-shift keying
DQPSK	differential quadrature phase-shift keying
FFT	fast Fourier transform
FPGA	field-programmable gate array
GPS	global positioning system
I/Q	in-phase and quadrature
LPI	low probability of intercept
NC-DQPSK	non-coherent differential quadrature phase-shift keying
PDF	probability density function
PSD	power spectral density
QPSK	quadrature phase-shift keying
RCR	radar-to-communications ratio
RDM	range-Doppler map
RF	radio frequency

SER symbol error ratio

SNR signal-to-noise ratio

SRBR symbol-rate-to-bandwidth ratio

Acknowledgments

I would like to acknowledge my thesis advisors, Dr. Romero and CDR Staples. Thank you for your support and guidance throughout the research and writing process.

To FRC team 5104, Breaker Bots, a sincere thank you for teaching me the practical application of the engineering knowledge I have been learning.

I would also like to thank the congregation of Covenant Presbyterian Church for their kindness and community, especially the Akin families. Your hospitality and willingness to welcome me into your homes has been such a blessing during this year.

Finally, to my parents, thank you for always being there for me, even when I was complaining about self-inflicted busyness brought about by procrastination. Thank you also for the foundation you provided that has enabled me to make it to this point. I wouldn't be here without your love and encouragement.

THIS PAGE INTENTIONALLY LEFT BLANK

CHAPTER 1:
Introduction

In the widest sense, this thesis is a continuation of previous efforts to better understand the maritime cyber environment; thus, a brief introduction to this concept is required. This work fits more specifically into previous efforts to determine the interaction between a communications signal and a radar signal occupying the same frequency band. Without the knowledge that others have investigated the feasibility of receiving and demodulating communications located in the same frequency band as high-powered radar, it makes little sense to consider the effect of relatively low-power communications signals as a specific type of interference that may be encountered by radar; however, this introductory information should suffice to illustrate to the reader why the effect of a communications signal on radar performance is a topic worthy of special study.

1.1 Maritime Cyber Domain

When considering how best to maneuver in a particular area of warfare, a terrain map is necessary in order to understand the environment and to be significantly effective while avoiding giving an advantage to the adversary. For instance, in submarine warfare, charts of the bottom of the ocean are used to avoid collision with any geographic features present. In the maritime cyber domain, such an understanding of the environment allows for both a greater understanding of our own vulnerabilities and possible ways to exploit adversary weaknesses. Examples of some of the signals that may be encountered in a maritime environment are navigational radar, fire control radar, communications between vessels, satellite communications, automatic identification system (AIS), global positioning system (GPS) and more. Additionally, ships have internal networks that allow systems such as voyage information sensors and engineering plant networks to communicate. These examples illustrate that there are many electromagnetic signals in the radio frequency (RF) spectrum on and off ships as well as internal networks within ships; thus, a robust understanding of how these different signals interact with each other is a crucial part of successful cyber operation at sea.

While there is no shortage of systems to investigate in this domain, in this thesis research

we focus on the effects on radar performance of the interaction between pulsed radar and communications systems. This selection was based on the ubiquity of pulsed radar and communications systems in the maritime environment and the potential to better utilize the potentially large amount of bandwidth used in radar systems.

1.2 Applications

We chose two applications to consider as motivation for why radar and communications signals might exist in the same frequency spectrum in the maritime environment: unintentionally through co-channel interference and intentionally by embedding one or more communications signals in the radar return.

1.2.1 Co-channel Interference

As communications systems consume more bandwidth, it is possible that they will start to utilize the S-band of around 3 GHz, where many maritime radars operate [1]. The two broad categories for how these two signals could be separated from each other can be classified as either cooperative, where each signal is designed and transmitted in a way that is intended to reduce interference, or non-cooperative, where neither the radar nor the communications system is modified to reduce interference. This kind of in-band interference has been previously studied, and cooperative strategies for reducing the frequency-domain overlap through radar pulse shaping were proposed [2]. The power spectral densities of a communications signal (top) and a radar signal designed to reduce interference with that communications signal (bottom) are shown in Figure 1.1. As shown in Figure 1.1, in-band interference is reduced by placing the majority of the radar pulse's energy outside the main lobe of the communications signal. This result is the outcome of a cooperative strategy for reducing frequency-domain overlap.

In contrast to the cooperative approach, we investigate a non-cooperative approach to interference cancellation, where each signal is recovered through post-processing instead of waveform design. Instead of spectrally shaping the radar or communications pulses to reduce interference, we use a rectangular envelope for both signals in the time domain. Additionally, we consider the scenario where there is no time multiplexing and instead assume that both the radar and communications pulses are active at the same time. The

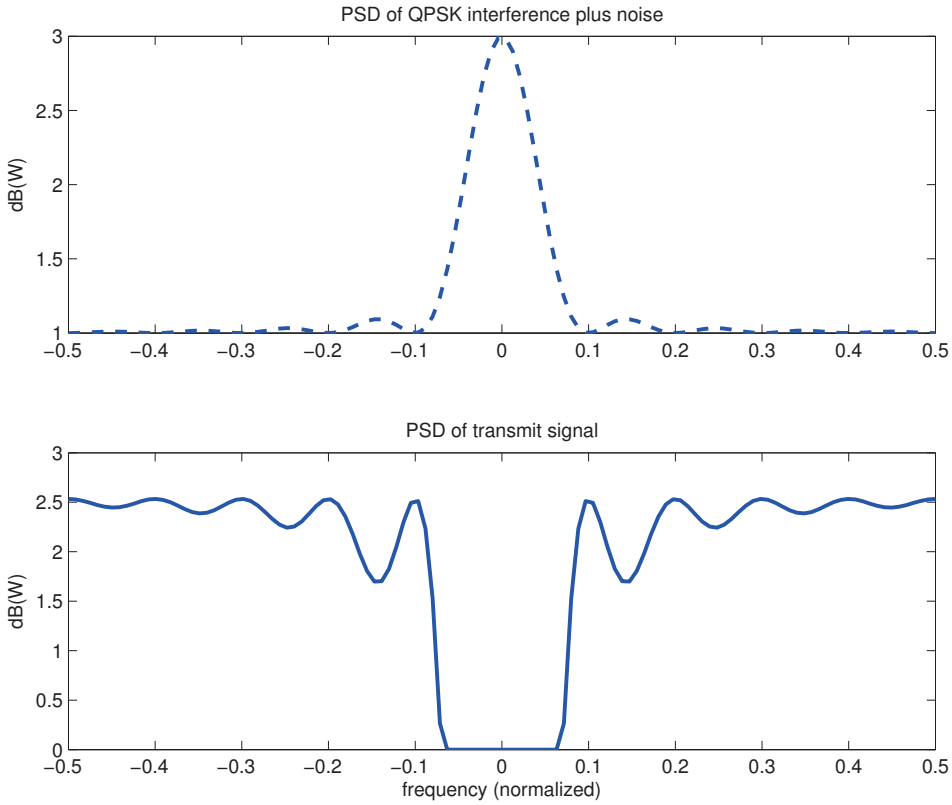

Figure 1.1. An Illustration of Pulse Shaping, to Reduce Interference. Source: [2].

signal model that describes this scenario is discussed in more detail in Chapter 2.

1.2.2 Embedded Communications

Another potential application of transmitting radar and communications signals in the same frequency band is to embed communications signals in the radar waveform or radar return. In this work, we draw inspiration from the traditional low probability of intercept (LPI) techniques of low power and phase-code modulation that are intended to prevent interception of a signal; however, in this case, the LPI-like quality of the communications signal is achieved by transmitting the communications signal in a location in time, space, and frequency that one does not expect to contain communication or even be able to successfully transmit information. For the purposes of this thesis research, the term LPI refers to low-power communications signals that are intentionally embedded in radar pulses and not the low power and phase-code modulation traditionally used for LPI signals.

The technique of embedding a communications signal within a radar pulse has been studied before, both in its cooperative and non-cooperative forms [3]–[5]. One cooperative method proposed suggests interpulse communication where the communication waveforms are specifically constructed as non-dominant eigenfunctions of the radar signal itself [3]. This approach requires new communications waveforms to be designed, so common digital modulation techniques such as phase-shift keying, frequency-shift keying, or amplitude-shift keying cannot be used [3]. In this work, we choose to investigate the effect of a modulation technique already commonly in use, specifically quadrature phase-shift keying (QPSK). Of course, other typical modulations can be used, but we use QPSK for illustration and simulations for reasons that are discussed further in Chapter 2. In this thesis, we assume the communications signal's presence is masked by its relatively low power compared to the radar power instead of by specifically-designed modulation schemes. This masking effect is illustrated in Figure 1.2. In this image, the top graph shows an example of the in-phase

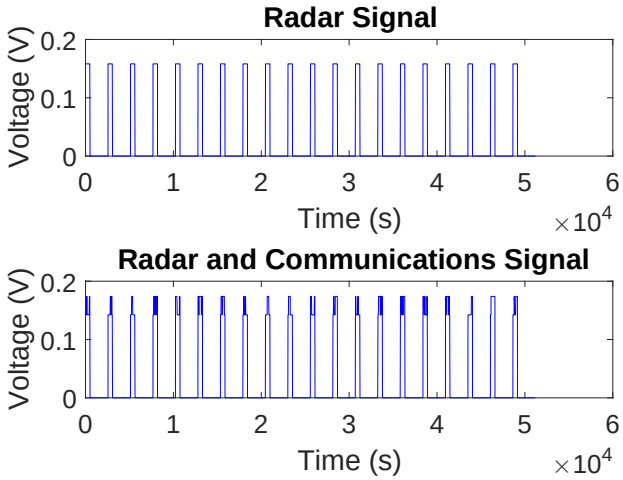

Figure 1.2. A Comparison of the Unaltered Radar Signal and the Combined Radar and Communications Signal

baseband component of a radar signal in the time domain without embedded communications. The bottom graph shows a relatively low-power communications signal embedded in the radar only during the time when a particular radar pulse is active. The presence of the embedded communications signal is visible as a fluctuation in signal amplitude while the radar is on. Since the radar signal power is much larger than the communications signal power (in this case, 20 dB larger), the presence of the communications signal is

effectively embedded within each radar pulse, which is why this communications signal is both embedded and intrapulse.

The particulars of how exactly this communications signal can be embedded within the radar pulse are outside the scope of this thesis research. Several options for where the signal can be inserted are possible. For instance, the transmitted radar pulse can contain a communications signal that is received by whatever target the radar was illuminating, although presumably only detected and demodulated by the intended party. In another scenario, illustrated in Figure 1.2, the communications signal can be embedded within the reflected radar return coming from another ship [4]. In this scenario, a ship at STA-1

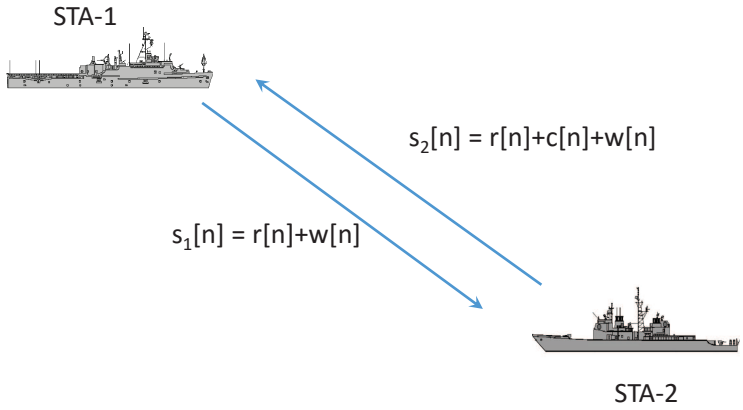

Figure 1.3. A Possible Scenario In Which Embedded Intrapulse Communications Could Be Used As an Embedded Communication Method. Source: [4].

illuminates a ship at STA-2 with its radar. The equation $s_1[n] = r[n] + w[n]$ represents the transmission by the ship at STA-1 of a signal plus noise. In this example, n is the discrete-time sample index, $r[n]$ refers to the radar pulse, and $w[n]$ refers to the noise. The LPI communications signal is embedded by the ship at STA-2 within the return from the radar signal, which is represented by the equation $s_2[n] = r[n]+c[n]+w[n]$. The additional $c[n]$ term in the return equation indicates the presence of embedded communications [4]; however, in each case, the performance of the radar is affected in equivalent ways given the same communications signal parameters at the radar receiver.

1.3 Objective

The background information provided above should be sufficient to demonstrate the need to investigate and quantify radar performance in the presence of an interfering communications signal as this environment is one that could easily be encountered, either intentionally or inadvertently, in the maritime cyber environment. Additionally, in the case of an intentionally embedded communications signal, we want to further validate the claim that this communications system is LPI-like in the sense we discussed previously; thus, in this thesis, we present several methods by which the effect of the embedded communications on radar performance can be determined. Of these methods, three are qualitative (power spectral density, range-Doppler maps, and navigational radar perspective) and one is quantitative (probability of detection). This analysis is carried out both through software simulation using MATLAB and hardware verification using System Generator and a field-programmable gate array (FPGA).

1.3.1 Thesis Outline

In order to meet the foregoing objective, the remainder of this thesis is organized in the following manner. Research previously performed in this area of radar and communications signals in the same frequency band, including the mathematical model used for the radar and communications signals, is presented in Chapter 2. The method and results from modeling the power-spectral density (PSD) is demonstrated in Chapter 3, followed by a similar analysis of probability of detection in Chapter 4. Range-Doppler maps (RDM) are investigated in Chapter 5, and the perspective of a radar operator in a maritime environment is considered in Chapter 6. Finally, conclusions and recommendations for future work are presented in Chapter 7.

CHAPTER 2:
Background

The work reported previously with regard to radar and communications signals operating in the same band must be understood in order to set the context for the effects of communication signals on radar performance. First, the justifications for using QPSK as the modulation technique and feasibility of recovering and demodulating the communications signal are discussed. Then, the mathematical model used for the radar and communications signals both in the background work and in this research is presented.

2.1 Modulation Technique Selection

Quadrature phase-shift keying was selected as the modulation technique for this thesis research to provide continuity with previous work. QPSK was analyzed using software simulation to assess the recoverability of the communications signal from the high-power radar interference [4]. QPSK is robust against a 1% error in frequency estimation, as seen in Figure 2.1. In this figure, symbol error ratio (SER) is parameterized by the symbol energy

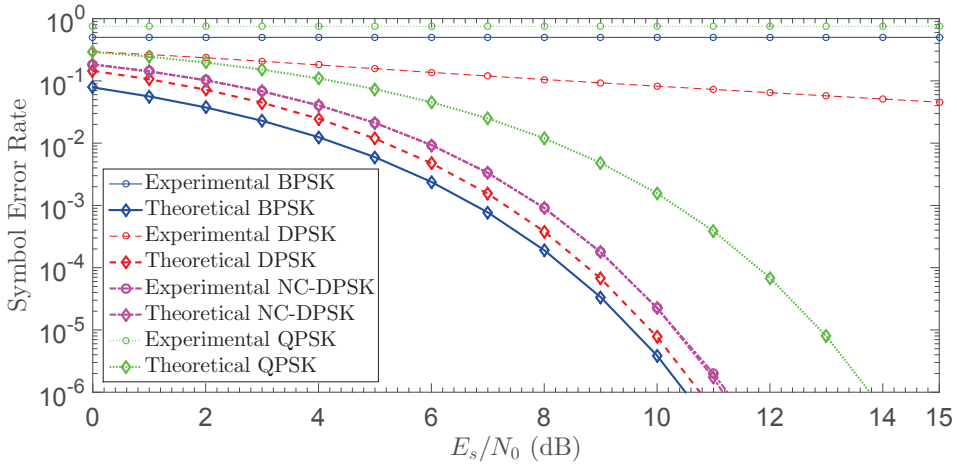

Figure 2.1. The SER Graph For Various Modulation Techniques With a 1% Frequency Estimation Error. Source: [4].

divided by the noise power spectral density. Differential QPSK (DQPSK) was found to

perform well in environments where the parameters of the radar signal were estimated given some error variance and, thus, not subtracted perfectly from the communications signal before demodulation. This superior performance is due to the ability to use non-coherent detection for differentially-coded signals, so errors in phase and frequency estimation have a smaller effect on SER.

While binary phase-shift keying (BPSK) and differential phase-shift keying detected both coherently (DPSK) and non-coherently (NC-DPSK) have a better SER for a given symbol energy to noise power spectral density (E_s/N_0), their throughput is half that of DQPSK since each DQPSK symbol encodes two bits of information. Since both DQPSK and QPSK have the same constellation diagram and PSD and differ only in how the data being transmitted is encoded before mapping the bits to symbols, the signals transmitted for both DQPSK and QPSK are indistinguishable even though the encoded bits may be different. For the purposes of radar performance as considered in this thesis, there is no difference between interference from DQPSK and interference from QPSK. The constellation diagram for both QPSK and DQPSK is seen in Figure 2.2, where the two axes x_1 and x_2 represent the in-phase and quadrature components of the baseband signal, respectively [6]. The way incoming

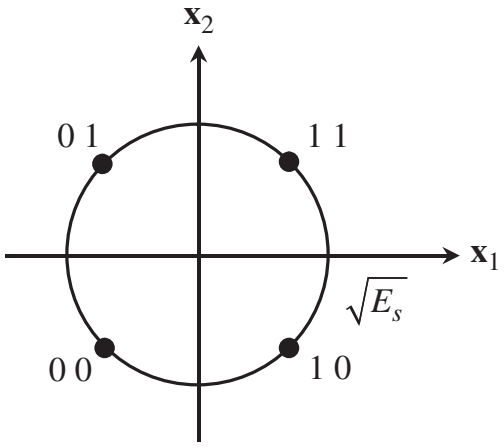

Figure 2.2. The Constellation Diagram For QPSK and DQPSK. Source: [6].

bits are mapped to in-phase and quadrature (I/Q) samples is identical in both cases, but in DQPSK pre-coding occurs before symbol mapping in order to properly encode not simply the original bit values but rather the differences between successive symbols.

2.2 Recoverability of Communications Signal

If the communications signal cannot be successfully extracted from the radar signal and demodulated with a sufficiently low bit error ratio (BER), then there is no reason to study the effect of communications on radar performance in the context of a LPI communications. The work referenced in [4] performed software simulations in order to determine the theoretical SER for various modulation techniques for a communications signal extracted from a radar signal through radar parameter estimation and cancellation; however, a different source performed hardware verification to ensure these simulation results could be replicated on an FPGA [5]. It can be seen from Figure 2.3 that radar estimation and cancellation using an FPGA can produce SER curves parameterized by E_s/N_0 that converge to the ideal curve as the number of radar pulses used to estimate the radar parameters increases. In order to

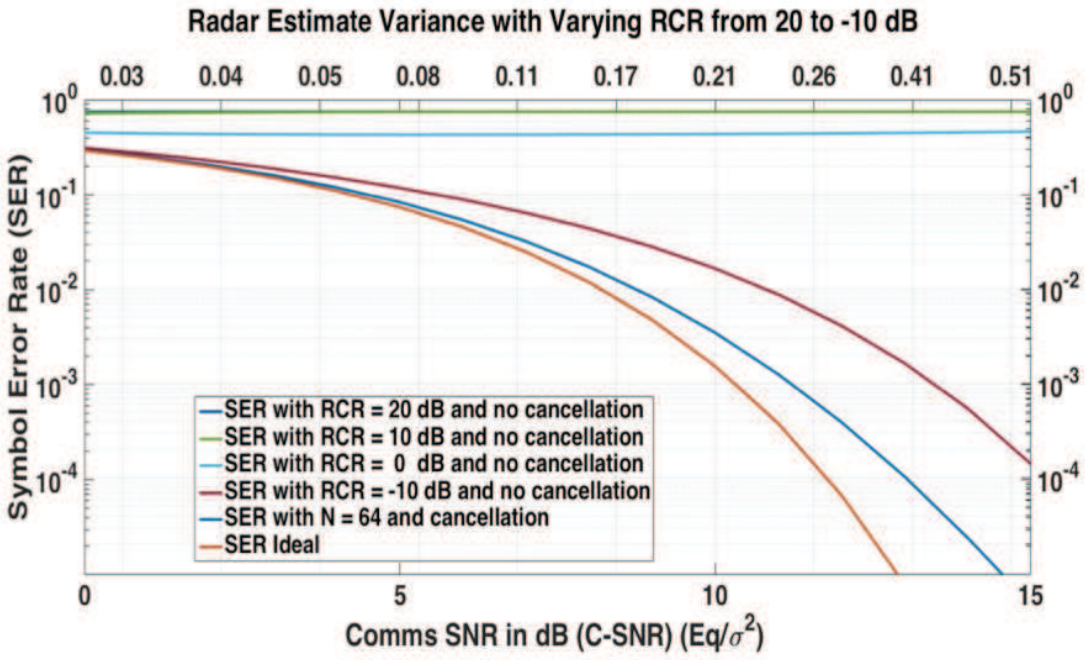

Figure 2.3. The SER Graph For Hardware-Based Radar Cancellation. Source: [5].

produce the SER curve shown in Figure 2.3, QPSK was used as the modulation technique; thus, we conclude that performing cancellation of the radar signal in order to recover and demodulate the transmitted communications signal in hardware is a viable technique. Since this potential communications method has been shown to be feasible in hardware in

terms of SER, its effect on radar performance must be considered before it can be further implemented.

2.3 Signal Model

Following from previous work such as [4], [5], we assume a complex-valued signal model such that the signal received at the radar receiver is $y(t) = r(t) + q(t) + w(t)$ where $r(t)$ is the radar signal, $q(t)$ is the communications signal that interferes with the radar, and $w(t)$ is zero-mean additive white Gaussian noise (AWGN). As with convention, signal processing occurs after analog-to-digital (A/D) sampling, so we now assume a discrete signal model with sampling frequency at least twice the Nyquist frequency. Additionally, we assume normalized sampling time where $T_S = 1$; therefore, the model is

$$y[n] = r[n] + q[n] + w[n], \tag{2.1}$$

where $n = 0, 1, 2, \ldots$ We assume a coherent pulse train waveform. The complex-valued radar baseband signal is given by

$$r[n] = \frac{1}{\sqrt{N}} \sum_{k=0}^{N-1} A_r e^{j\phi_r} u_n[n - kT_r], \tag{2.2}$$

where A_r is the amplitude of the radar signal, ϕ_r is the phase of the pulse, and the sum $\sum_{k=0}^{N-1} u_n[n - kT_r]$ is a rectangular pulse train consisting of N pulses where T_r is the pulse repetition interval, and $u_n[n]$ is given by

$$u_n[n] = \frac{1}{\sqrt{t_p}}(u[n] - u[n - t_p]), \tag{2.3}$$

where $u[n]$ is the standard unit step function and t_p is the time in which a pulse is active. If $A_r = 1$, then the pulse train in Equation 2.2 is of unit energy; thus, A_r serves to scale the radar signal to the desired energy. The duty cycle of the radar can be expressed as $D = t_p/T_r$. The communication signal is modeled as a QPSK complex signal with amplitude A_q which is given by

$$q[n] = \frac{A_q}{\sqrt{N}} \sum_{k=0}^{N-1} u_c[n - kT_r], \tag{2.4}$$

where $u_c[n]$ is defined as

$$u_c[n] = \frac{e^{j\phi_q}}{\sqrt{t_p}}(u[n] - u[n - t_p]). \tag{2.5}$$

The symbols are a random draw from the set $\phi_q \in \left[\frac{\pi}{4}, \frac{3\pi}{4}, \frac{5\pi}{4}, \frac{7\pi}{4}\right]$. If $A_q = 1$, then the waveform described by (2.4) is of unit energy; thus, A_q serves to scale the energy desired for this communications signal. The amplitude of the QPSK symbols is set by the power ratio of the radar signal and embedded communications signal (defined as RCR); thus, RCR in dB is defined as

$$RCR_{dB} = 10\log_{10}\left(\frac{P_r}{P_q}\right), \tag{2.6}$$

where P_r and P_q are defined above as the power of the radar and communication signals, respectively. Actual $RCR = P_r/P_q$. Since the communications signal is only present when the radar pulses are on, the RCR simply becomes an energy ratio:

$$RCR_{dB} = 10\log_{10}\left(\frac{A_r^2}{A_q^2}\right). \tag{2.7}$$

The values of the RCR_{dB} explored in this thesis range from a maximum of 20 dB to a minimum of 3 dB.

One important consideration is the effect of changing symbol rate (i.e., data rate) to the radar spectrum (if spectrum is used for LPI considerations). Here, we mean the symbol rate to be the rate during the radar pulse's on-time. Clearly, the effective data rate is reduced by the duty cycle, but since we intentionally do not embed during the pulse's off-time, this reduction does not affect our intended data rate. For convenience, the symbol rate may be normalized by the radar pulse rate (or bandwidth). We call this value the symbol-rate-to-bandwidth ratio (SRBR). The SRBR determines how many QPSK symbols are transmitted during the duration of one radar pulse. If we let $R_s = 1/T_s$, where T_s is the symbol duration, and let the radar bandwidth be $B_r = 1/t_p$, then SRBR can be expressed as:

$$SRBR = \frac{R_s}{B_r}. \tag{2.8}$$

The values for SRBR used in this thesis range from one symbol per pulse to 512 symbols

per pulse. In our various investigations of the effects of the embedded intrapulse communications on radar performance, we parameterize the communications signal by both the RCR and the SRBR.

In order to illustrate the effect of changing these parameters on the combined radar-communications signal, a sample of the in-phase component of the signal at baseband is plotted. In Figure 2.4, the SRBR is held constant at eight while the RCR is changed from a relatively large value of 20 dB to a relatively low value of 10 dB. In both cases,

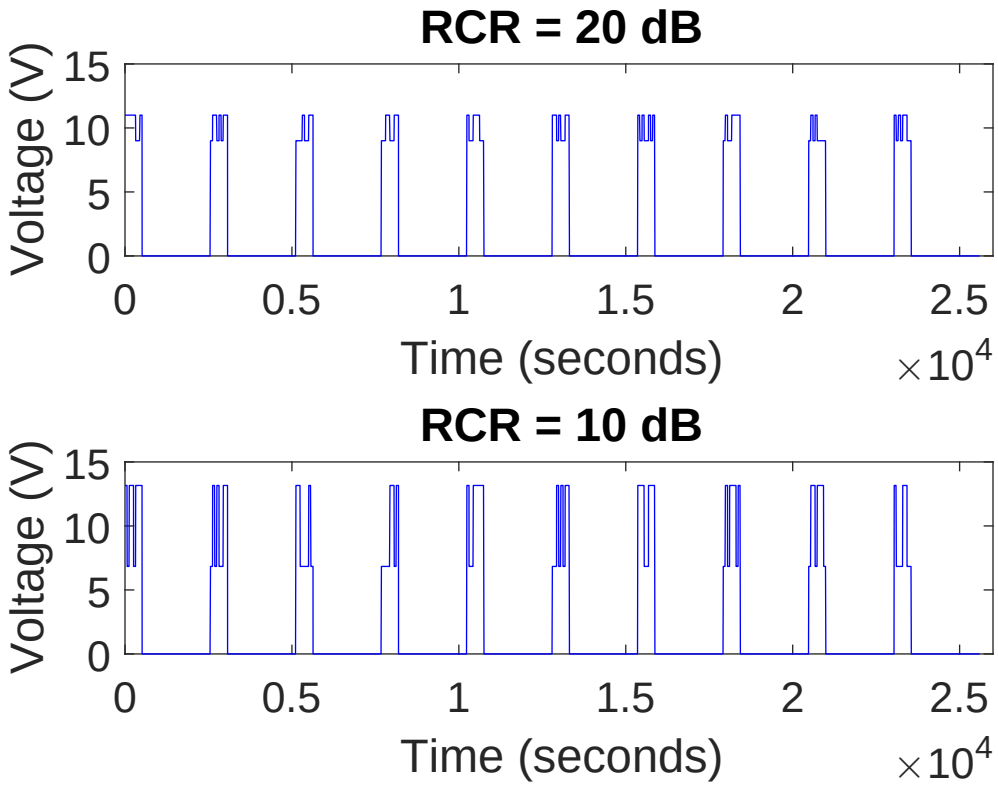

Figure 2.4. The Effects of Varying the RCR On the In-Phase Component of the Time-Domain Signal

the amplitude of each radar pulse without the embedded communications is 10 V. In the top plot, when the RCR is 20 dB, the communications signal only adds or subtracts 1 V from the amplitude of the radar signal. In the bottom plot, when the RCR is 10 dB, the communications signal adds or subtracts 3.16 V from the amplitude of the original radar signal. This difference is easily visible when looking at the two signals, as the 10 dB case

has a much greater variation in amplitude while the radar is on than the 20 dB case does; thus, we hypothesize that varying the RCR has a large effect on radar performance, so this is a parameter that must be investigated.

In Figure 2.5, the RCR is held constant at 10 dB while the SRBR varies from a relatively large value of 64.0 to a relatively small value of 2.0. While the total time for a given radar

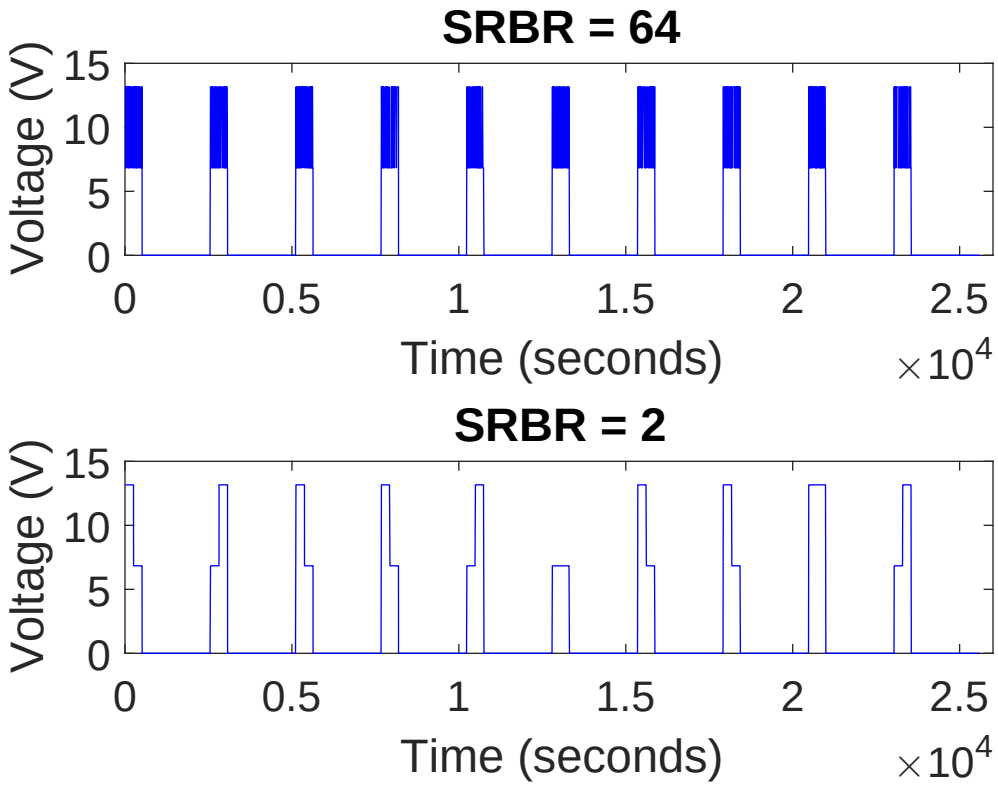

Figure 2.5. The Effects of varying the SRBR On the In-Phase Component of the Time-Domain Signal

pulse is the same in each case, in the high-SRBR case the QPSK symbol time is one-sixty fourth the radar pulse duration, and in the low-SRBR case the QPSK symbol time is one-half the radar pulse duration. As in the case where RCR was varied, these dramatic differences in SRBR are easily visible just by looking at the time-domain plots of the signals. In the top plot, when the SRBR is equal to 64.0, the individual symbols are difficult to discern since there are so many symbols in each relatively-short radar pulse. However, in the bottom plot, when the SRBR is equal to 2.0, the individual symbols are visible. While changing

SRBR does cause some visible fluctuation, as shown above in the radar in-phase signal, the fluctuations are almost non-existent when the combined radar and communications signal's magnitude is considered. Especially if an energy detector is used in the radar receiver instead of a matched filter detector, these small fluctuations will have little, if any, effect on radar performance. Varying the number of QPSK symbols per radar pulse does have the potential to make the frequency-domain representation of the combined radar and communications signal more similar to that of the radar signal alone, thus reducing the effect of embedded communications. Additionally, the effect on probability of detection, range-Doppler maps, and navigational radar from a varying SRBR must be considered as well.

We now consider the frequency-domain representation of embedded communications signals with varying RCR and SRBR values by generating and analyzing PSDs for these signals through software simulation.

CHAPTER 3:
Power Spectral Density

The first metric used to analyze the effect of the communications signal on radar performance is the PSD of the combined radar and communications signal compared to the PSD of the radar signal alone. While understanding the signal in the time domain is important, the effects of embedded intrapulse communication on the radar spectrum must be considered as well.

3.1 Theory

Power spectral density is analogous to the Fourier transform but is used for random signals, where the Fourier transform is defined for deterministic signals. The PSD is defined for a signal $X(t)$ as

$$S_{XX}(f) \equiv \lim_{t_o \to \infty} \frac{\mathbb{E}[\mid X_{t_o}(f) \mid^2]}{2t_o}, \tag{3.1}$$

where $X_{t_o}(f)$ is the Fourier transform of the signal $X(t)$ truncated between time $t = -t_o$ and time $t = t_o$ [7]. One challenge in determining the spectrum utilization for the radar signal with embedded communications is the intrapulse nature of the communication system. In this case, QPSK symbols are not transmitted continuously but rather only during the radar's t_p time. The closed-form power spectral density (PSD) for baseband QPSK with pauses matching a radar duty cycle has not been well-defined to our knowledge. Instead of determining a closed-form expression for the PSD, we instead rely on signal simulation in order to illustrate the PSD of the radar pulse, with and without embedded communications.

3.2 Software Simulation

In the discrete time environment, we use the discrete Fourier transform implemented using the fast Fourier transform (FFT) algorithm and modify the equation used to determine PSD to

$$S_{XX}(f) = \frac{f_s \mid \mathbb{F}\{X[n]\} \mid^2}{M}, \tag{3.2}$$

where f_s is the sampling frequency used to convert the signal from continuous time to discrete time and M is the FFT size. In all of our analyses, we use a normalized sampling frequency equal to 1 Hz. Our FFT size is chosen to be the next highest power of two greater than the length of the signal L in order to maximize the efficiency of the FFT algorithm; thus,

$$M = 2^k, \tag{3.3}$$

where M is the smallest value that satisfies $M > L$ for an integer value of k. In all cases, we use a rectangular pulse shape for both the radar signal and the QPSK signal. Other pulse shapes, for instance a Hamming pulse shape for the radar signal or a raised cosine pulse shape for the communications signal, are possible, but using a rectangular envelope pulse shape allows us to investigate the largest anticipated spectral occupancy for these signals without pulse shaping. The PSD of the radar pulse alone is shown in Figure 3.1 to provide a basis for comparison with the radar signals with embedded communications that are presented later in this chapter. In order to generate the PSD shown in Figure 3.1,

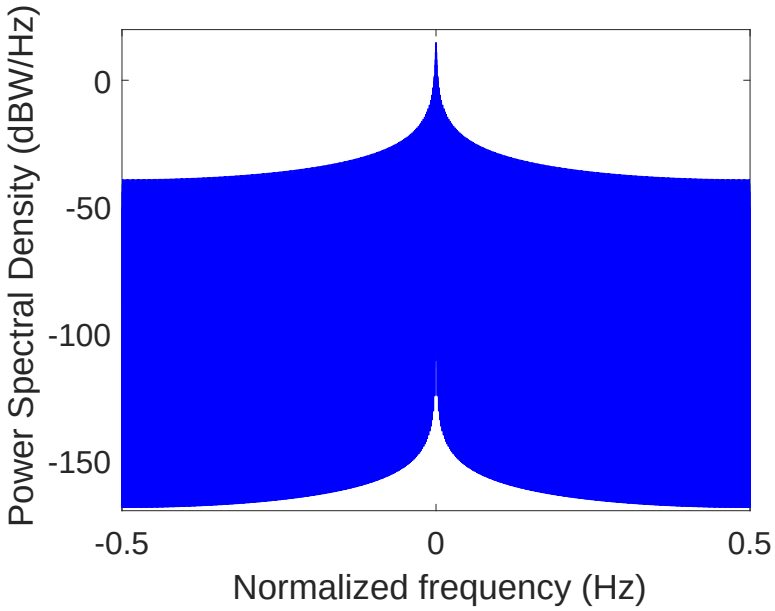

Figure 3.1. The PSD of the Original Radar Signal

we utilized $N = 1000$ radar pulses with a duty cycle of 10%. The radar phase used was $\phi_r = \pi/4$. We use these radar parameters, while varying RCR and SRBR, for all other PSD plots shown in this chapter.

3.2.1 Varying RCR

To compare radar and communications PSDs, we first vary the RCR. As mentioned previously, the same radar parameters were used that were set for Figure 3.1. Additionally, SRBR = 1 is used. Since there is only one QPSK symbol with a rectangular pulse shape embedded in each radar pulse and the symbol time T_S for the QPSK signal is equal to the radar pulse time t_p, it is unsurprising that the shape of the communications signal in the frequency domain is identical to the shape of the radar signal in the frequency domain, differing only in magnitude. The PSDs for the communications signal alone at various RCR levels can be seen in Figure 3.2. In Figure 3.2, the RCR = 3 dB signal is plotted in blue, the RCR =

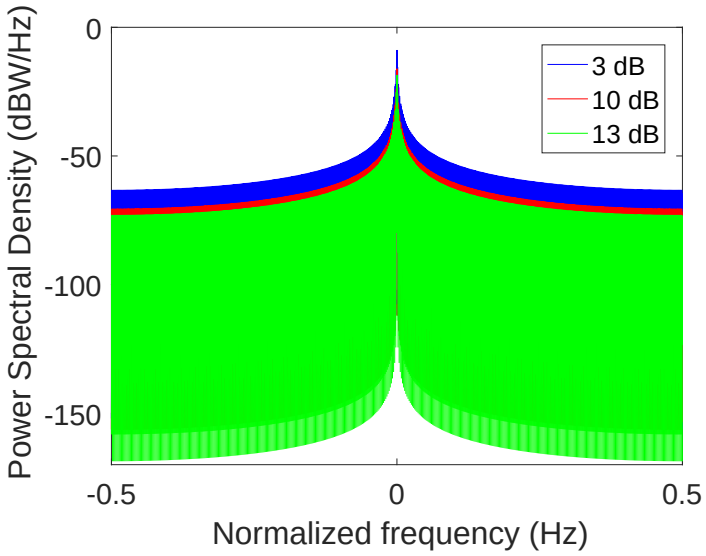

Figure 3.2. The PSD of the Communications Signal Alone at Various RCRs

10 dB signal is shown in red, and the RCR = 13 dB signal is shown in green. Since the radar amplitude is held constant, increasing the RCR results in a smaller amplitude for the communications signal. The RCR = 3 dB communications signal has the largest amplitude in Figure 3.2 since the power of the communications signal is approximately half that of the radar signal, while the power of the 13-dB signal is roughly one-twentieth the power of the radar signal, and so its amplitude is the smallest. Enlarging the figure in the center of the frequency domain allows us to see the characteristic shape of the sinc function, as we would expect for a signal with a rectangular pulse in the time domain. This enlargement is shown in Figure 3.3 using the same colors for the different RCR values as in Figure 3.2. Now that we have an understanding of what the PSDs for both the communications

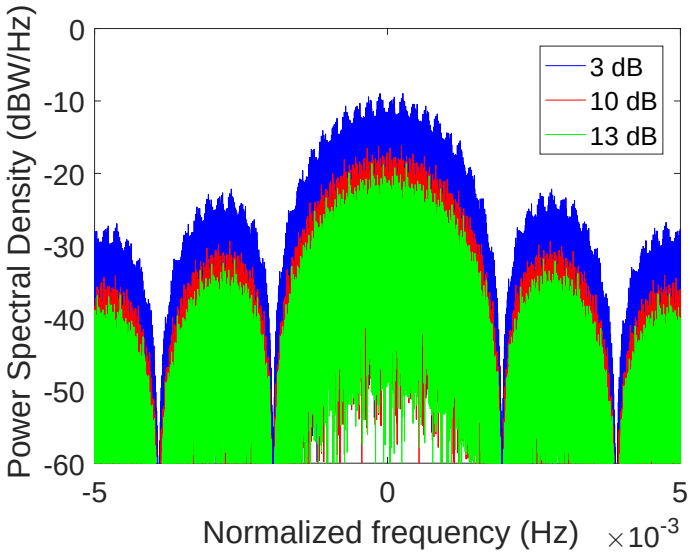

Figure 3.3. The Enlarged PSD of the Communications Signal Alone at Various RCRs

and radar signals look like, we can compare these results with the PSDs of the combined radar and communications signal at various RCRs. In order to evaluate how similar the radar and communications signal is compared to the communications signal alone in the frequency domain, we plot the PSDs on the same axes as the radar-only PSD so that the differences are more noticeable. These PSDs, as well as the differences between the radar signal and the combined radar and communications signal for each RCR value, are shown in Figure 3.4 for RCRs of 3 dB, 10 dB, and 13 dB. In Figure 3.4, in the left column, the PSD for the unaltered radar signal is plotted in red, and the PSD for the combined radar and communications signal is plotted in blue. Since the communications signal has the same pulse shape as the radar signal but with much less power, the difference between the PSDs of the radar signal alone and the combined signal is nearly indiscernible for even the highest RCR considered. In the right column of Figure 3.4, we plot the difference between the two spectra in the left column in order to better understand the effect of embedded communications on the PSD of the received signal. It can be seen from the right column that the differences between the two signals are incredibly small. For most of the spectrum, there is less than a -50-dB difference, which indicates remarkable similarity between the two signals. So, we see that changing the RCR to even relatively small values (therefore, relatively high-powered communications signals) still allows the communications signal to

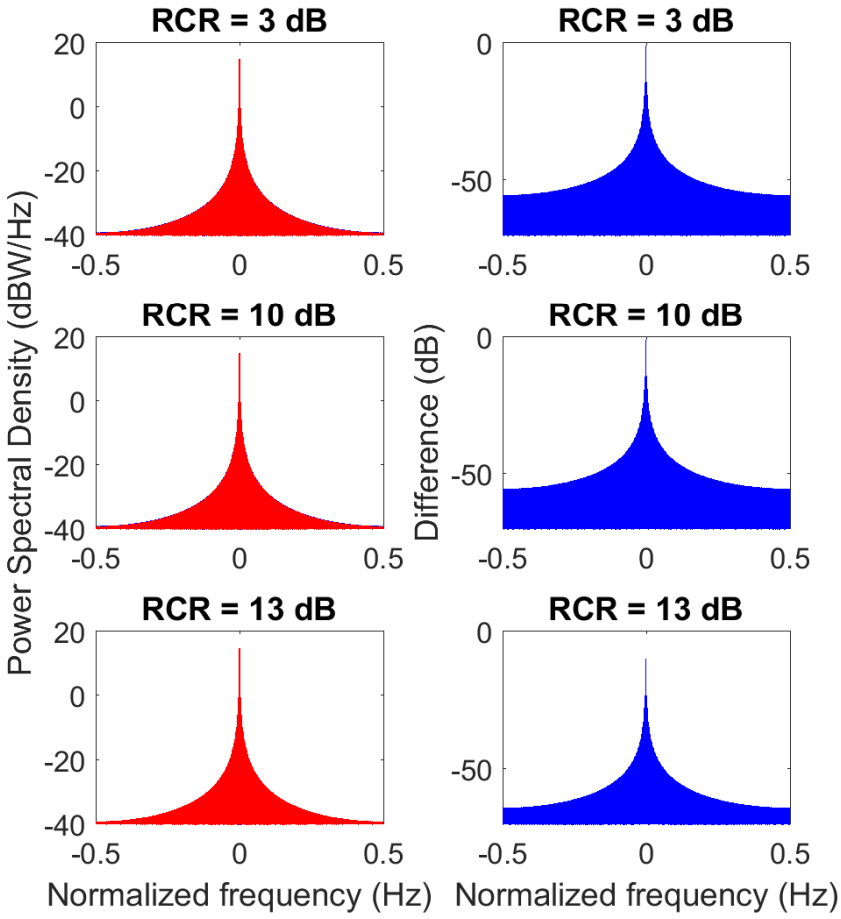

Figure 3.4. The PSDs and Differences between PSDs of the Radar Signal Only and the Combined Radar and Communications Signal for Various RCR Values

have little effect on the frequency spectrum of the combined radar and communications signal as long as the SRBR is equal to one.

3.2.2 Varying SRBR

We now fix the RCR at 10 dB and investigate the PSD of the received signal when the SRBR is varied, ranging from 1.0 for the smallest data rate to 512.0 for the largest. As we saw in the previous section, when the SRBR is equal to 1.0, the communications signal has a similar shape in the time domain and, therefore, the same PSD as the radar signal. We now plot

the PSDs of the communications signal alone with SRBR values of 1.0, 128.0, and 512.0 in order to better understand what these PSDs look like independent of the radar signal. While before we could plot our three example communications signals on the same axes and clearly see the differences since they all had the same pulse shape, we now must plot each communications signal on separate axes since they no longer have the same spectral shape. These different shapes are illustrated in Figure 3.5. For each of the SRBR values illustrated,

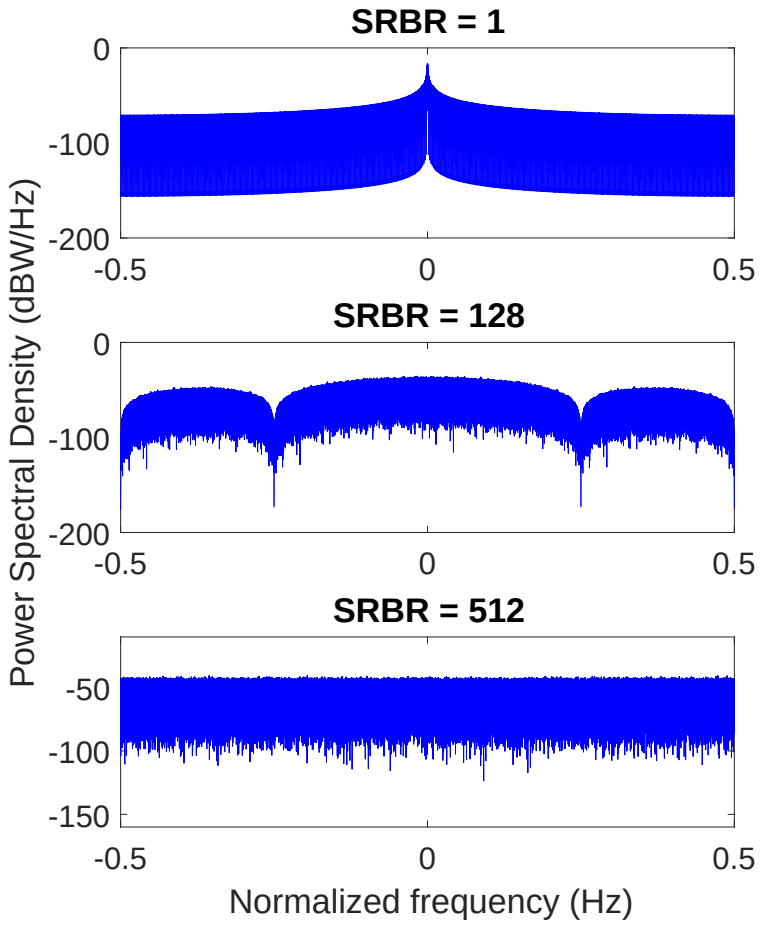

Figure 3.5. The PSDs of the Communications Signal Only with Various SRBR Values

the RCR is held constant, and the total energy contained in each signal remains the same. As the SRBR increases, a greater proportion of the signal's energy is contained within higher frequencies. As these increasing frequency components carry a larger proportion of

the communications signal's energy, the communications signal can no longer be spectrally contained within the PSD of the radar pulse. Now, we look at the PSDs of the combined radar and communications signal, again plotted on the same axes as the radar signal for comparison. These PSDs (shown in red) and the difference PSDs (i.e., the absolute value of the resulting subtraction of the combined radar and communications PSD and the radar-only PSD) are shown in Figure 3.6. In Figure 3.6, the left and right columns are organized as

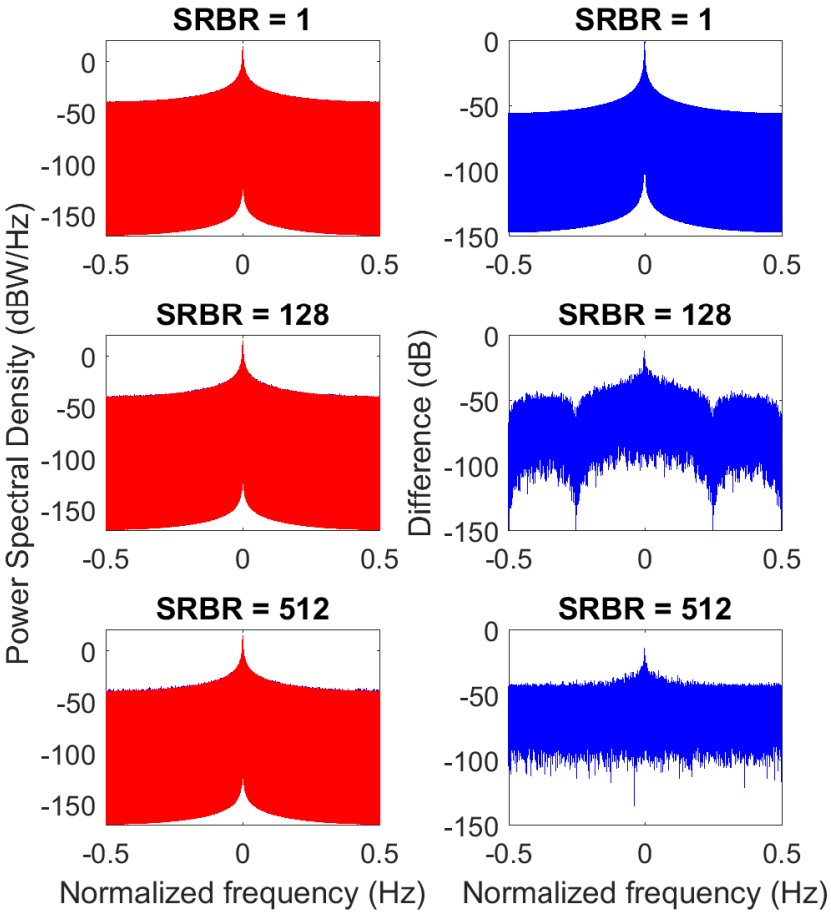

Figure 3.6. The PSDs and Differences between PSDs of the Radar Signal Only and the Combined Radar and Communications Signal for Various SRBR Values

they are in Figure 3.4. The conclusion that can be drawn from Figure 3.6 is similar to the conclusion drawn for the cases where the SRBR was held constant and the RCR was varied. As SRBR increases, the frequency-domain representation of the communications signal

becomes more and more different from the frequency-domain representation of the radar signal. At higher SRBRs, the differences between the radar-only signal and combined radar and communications signal are more visible; however, as illustrated by the difference PSDs in the right column, these differences are still relatively small. Now that we have validated that the embedded communications has a small effect on the frequency spectrum of the radar signal, we assess the radar probability of detection as a measure of radar performance.

CHAPTER 4:
Probability of Detection

Probability of detection is a measure of radar performance that is used to determine how often a radar correctly detects a target given a particular signal-to-noise ratio (SNR) environment and probability of false alarm P_{FA}. In this chapter, we first explore the theory behind radar probability of detection and then show the effects of embedded intrapulse communication on this metric of radar performance through both software simulation and hardware verification.

4.1 Theory

After the radar receives a signal, it must distinguish between a returned pulse and noise. A graph of possible distributions for both the returned pulse and noise is shown in Figure 4.1. Signal magnitude is shown on the x-axis, and the probability density function (PDF) for the

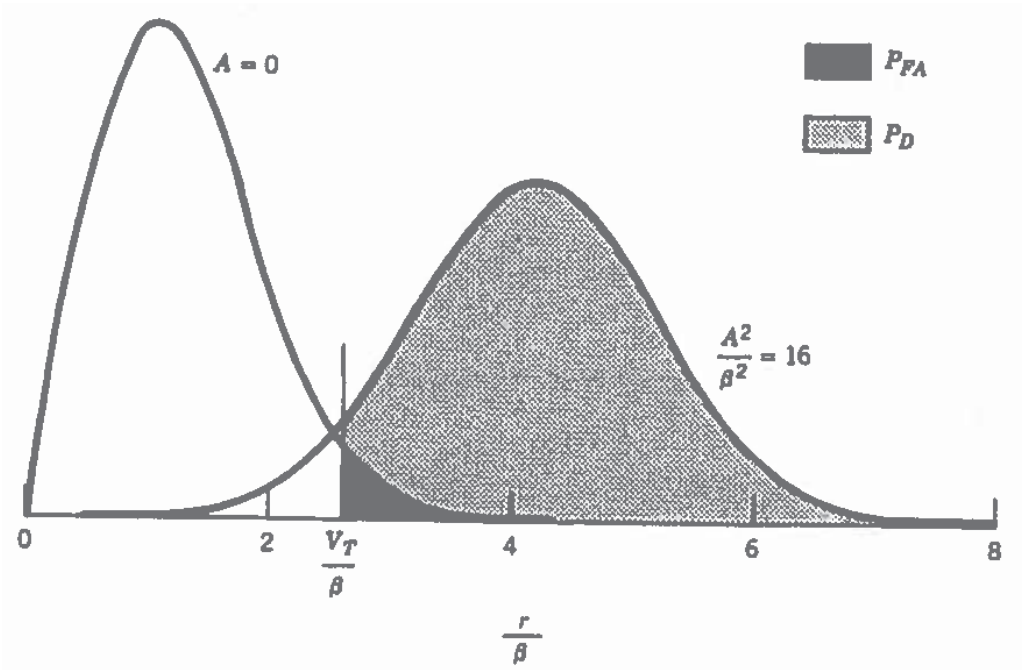

Figure 4.1. Probability Density Functions for Both Pure Noise (Left) and a Noise-Corrupted Returned Pulse (Right) in a Radar Receiver Using an Envelope Detector. Source: [8].

noise signal (on the left) or noise-corrupted returned pulse (on the right) is shown on the y-axis [8]. In this case, the distributions of each signal are a result of the detector, which utilizes a narrow band-pass filter and considers the magnitude of the complex-valued I/Q samples. The noise alone results in a Rayleigh distribution, while the radar signal with noise can be approximated by a Gaussian probability density function [8]. Since the two distributions overlap, it is impossible to successfully reject all false returns from noise signals while at the same time capturing every true target; therefore, probability of false alarm is used to set a threshold γ'. Received magnitudes greater than γ' are deemed target returns [9]. In Figure 4.1, this threshold is shown as the vertical line at an amplitude of approximately 2.5 for illustration [8]. The noise signals with a magnitude that exceeds the threshold are shown in black, representing the probability of false alarm. Since the total area under each PDF curve is equal to one, the area under the noise-magnitude distribution from the threshold to infinity is equal to P_{FA}. The area under the target-and-noise magnitude distribution shown in dark gray represents the probability of detection. If the P_{FA} is increased (which is usually not desired) by moving the threshold, the probability of detection is increased (which is usually desired); thus, a trade-off exists between P_{FA} and probability of detection. [8]. While P_{FA} values used in real-world scenarios vary based on the severity of the consequences of an incorrect decision, we use $P_{FA} = 0.01$ as a typical value in this thesis.

While the graph shown in Figure 4.1 was not generated using a matched filter receiver, the principles that can be derived from its example are applicable to the matched filter. In all further examples, we assume the return signal has passed through a matched filter designed to maximize the SNR of the radar pulse. Assuming matched filtering and AWGN, we can calculate the threshold γ' as

$$\gamma' = \sqrt{\frac{\sigma^2 E}{2}} Q^{-1}(P_{FA}), \tag{4.1}$$

where σ^2 is the variance of the Gaussian noise, E is the signal energy, and $Q^{-1}(\bullet)$ denotes the inverse Q-function [9]. Given a particular γ', the probability of detection can be calculated as

$$P_D = Q\left(Q^{-1}(P_{FA}) - \sqrt{\frac{2E}{\sigma^2}}\right), \tag{4.2}$$

where $Q(\bullet)$ denotes the Q-function, and all other variables have the same meaning as in Equation 4.1 [9].

Since the signal energy is a component of the probability of detection equation, we can plot the probability of detection against different SNRs for a P_{FA} value of 0.01 to illustrate the theoretical P_D in the absence of embedded intrapulse communications. This plot is shown in Figure 4.2. As expected, probability of detection is low when the SNR is small and

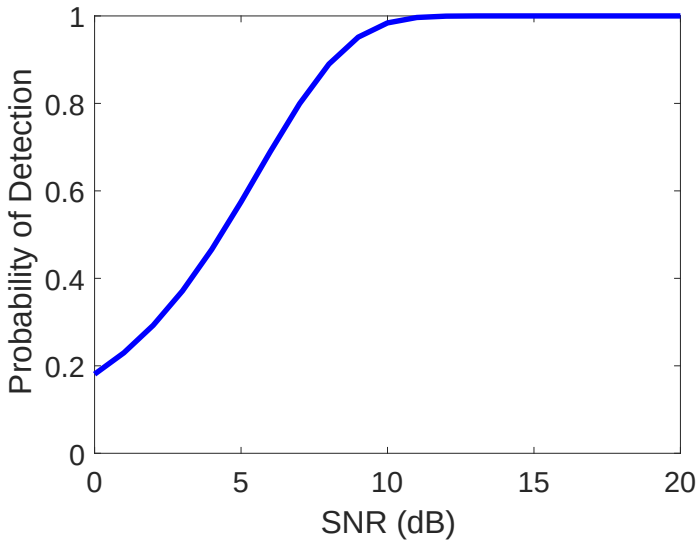

Figure 4.2. Theoretical Probability of Detection vs. SNR Curve without Embedded Communications

high when the SNR is large, approaching one at SNRs of about 10 dB or higher for this P_{FA} value. We now investigate the effect on probability of detection of adding embedded intrapulse communications to the radar signal.

4.2 Software Simulation

Software simulation was performed using a Monte Carlo simulation with a number of trials $N = 10^5$ in MATLAB. In order to determine detection probability, combined radar and communications signals were generated in MATLAB for various RCRs and SRBRs. The real part of the matched-filtered and sampled received signal was compared to γ', with a value greater than or equal to γ' corresponding to detection and a value less than γ' corresponding to classifying that trial as noise. Next, the number of times the signal was detected was divided by the number of trials in order to obtain an estimate of the probability of detection.

4.2.1 Varying RCR

As before when analyzing the PSD of the combined radar and communications signal, we begin by varying the RCR to see how it affects the radar detection performance. For these trials, the SRBR is fixed at 1.0 and the RCR is varied between 3 dB, 6 dB, and 10 dB. The results of these simulations are shown in Figure 4.3. When RCR increases, the probability

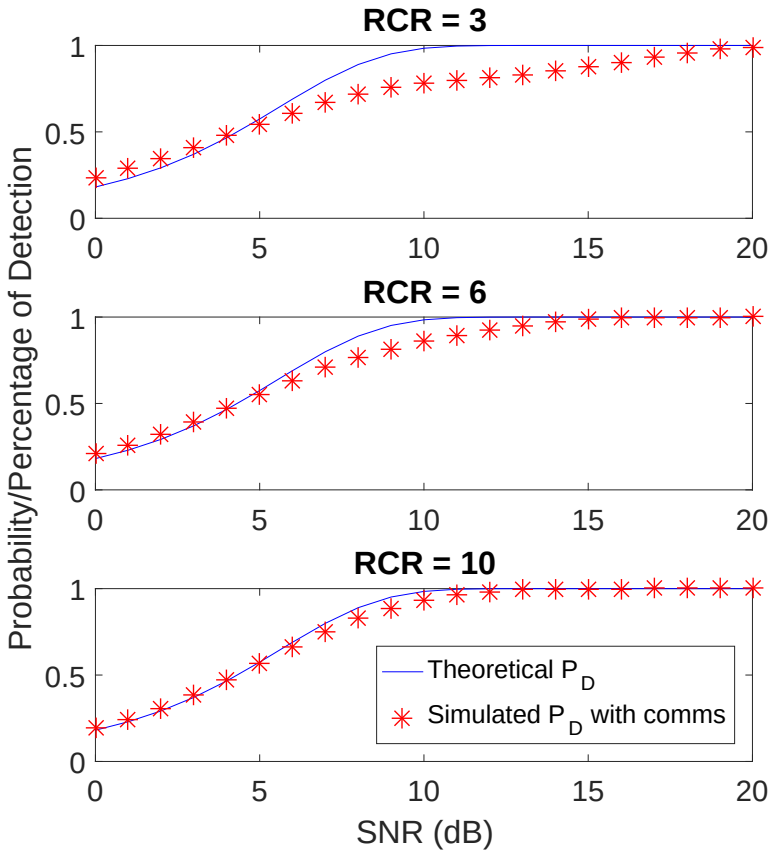

Figure 4.3. Probability of Detection for Various RCR Values

of detection of the radar signal with embedded communications approaches the probability of detection of the radar-only signal. With an RCR of 3 dB, there is a significant difference between the P_D of the combined radar and communications signal and that of the radar signal alone. Interestingly, not only is the performance worse than the performance of the radar-only signal for most of the SNRs investigated, which is expected, it is actually better for small SNRs. However, this difference all but disappears as the RCR is increased to 10 dB. This result makes sense, as increasing the RCR means that the communications signal

is smaller compared to the radar signal. When RCR is small, the interference effect of the communications signal to the radar signal becomes more significant, so the probability of detection of the radar is degraded.

4.2.2 Varying SRBR

Next, we fix the RCR at 3 dB and vary the SRBR in order to determine the effect of SRBR on the probability of detection of the radar. The results of these simulations are summarized in Figure 4.4. As shown in Figure 4.4, increasing the SRBR was found to cause the probability

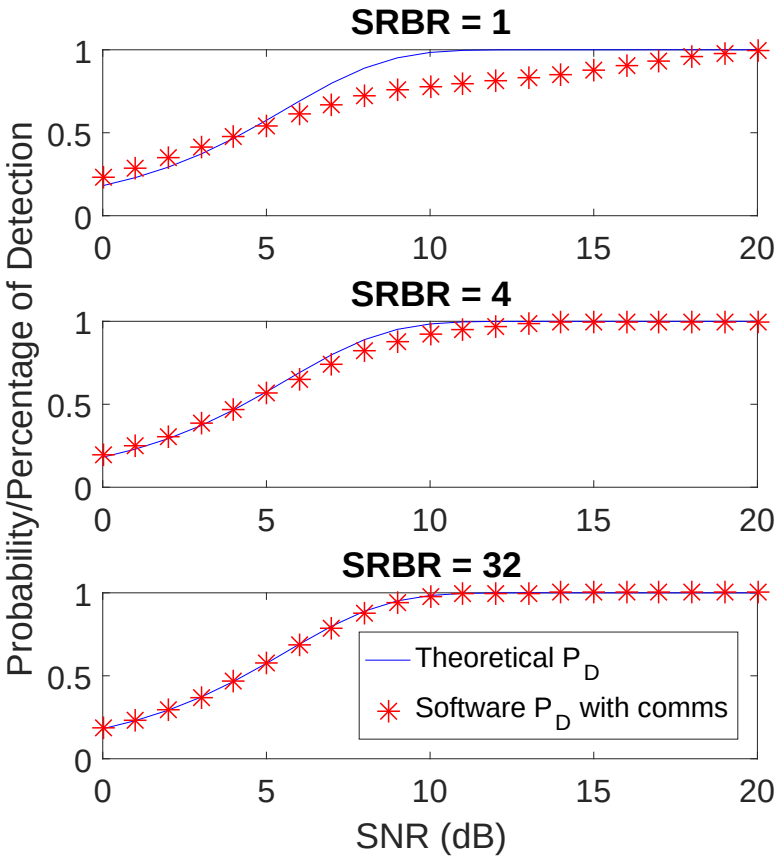

Figure 4.4. Probability of Detection for Various SRBR Values

of detection of the combined radar and communications signal to rapidly approach the probability of detection of the radar-only signal. At an SRBR of only 4 QPSK symbols per radar pulse, P_D is almost equivalent to the radar-only case, and at 32 QPSK symbols per

radar pulse, the P_D of the combined radar and communications signal is indistinguishable from the P_D of the radar-only signal. So, we conclude that increasing the SRBR decreases the effect of embedded intrapulse communications on pulsed radar performance because the resulting P_D approaches the theoretical radar detection probability.

4.3 Hardware Validation

In order to verify the results from software simulation, a simple radar receiver architecture was created using Xilinx System Generator and implemented on a Xilinx Kintex-7 FPGA. This FPGA is shown in Figure 4.5. An FPGA was used to simulate the architecture of a

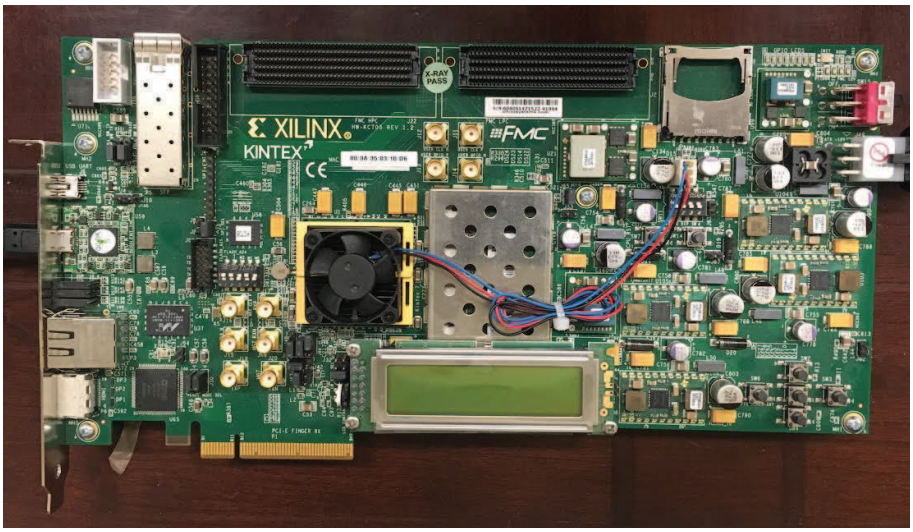

Figure 4.5. The FPGA Used for Hardware Validation

radar receiver. In fact, modern radar receivers are built using FPGAs, so while the hardware setup we used is not identical to that contained within a radar, it is very similar, and provides a good analog for how the radar receiver will perform with radar pulses with embedded communications. In order to validate the probably of detection in hardware, the signal generation and probability of detection algorithms were recreated in Simulink using System Generator blocks. The same RCR and SRBR values that were simulated in software were tested in hardware. The testing setup in Simulink is shown in Figure 4.6. As shown in Figure 4.6, the simulation is run on both the computer in Simulink, through the top signal path, and on the FPGA in a hardware description language, through the JTAG Cosim block, in order to verify FPGA performance is the same as the performance in Simulink. For the

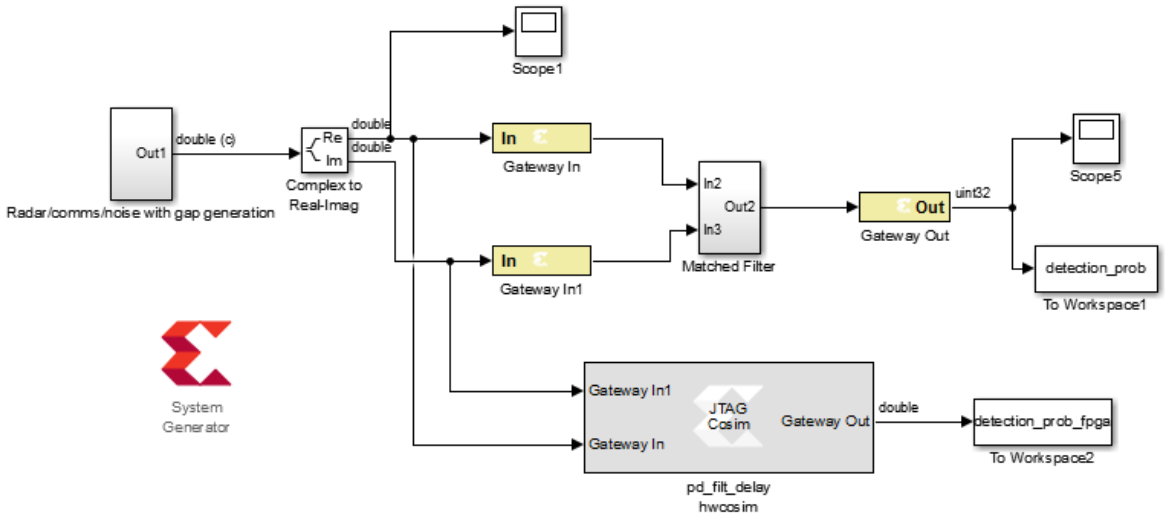

Figure 4.6. The Probability of Detection Hardware Test Setup in Simulink

hardware portion, $N = 10^3$ trials were used due to far greater computational complexity for the hardware validation than for the software simulation.

4.3.1 Varying RCR

To verify the probability of detection results at various RCR values, P_D was simulated on the FPGA using an SRBR of 1.0 and RCR values of 3 dB, 6 dB, and 10 dB. These results are shown in Figure 4.7. As shown in the plot, the hardware results align well with the software simulation. While the results are not identical, this difference is likely due to different methods of noise generation in Simulink and MATLAB. In Simulink, the AWGN is band-limited, while in MATLAB, there is no limitation placed on the Gaussian distribution used to generate the noise. The results from the FPGA validation indicate that the P_D results from a radar will likely be very similar to what we simulated.

4.3.2 Varying SRBR

Next, RCR is held constant at 3 dB and SRBR is varied to be 1.0, 4.0, and 32.0 to test the same scenario that was simulated in software. The P_D results for these parameters are shown in Figure 4.8. As with the case when RCR was varied, the hardware results are very similar to the simulation results. While there is a noticeable difference in probability of detection for the SRBR = 1.0 case, the hardware detection probability is virtually identical to

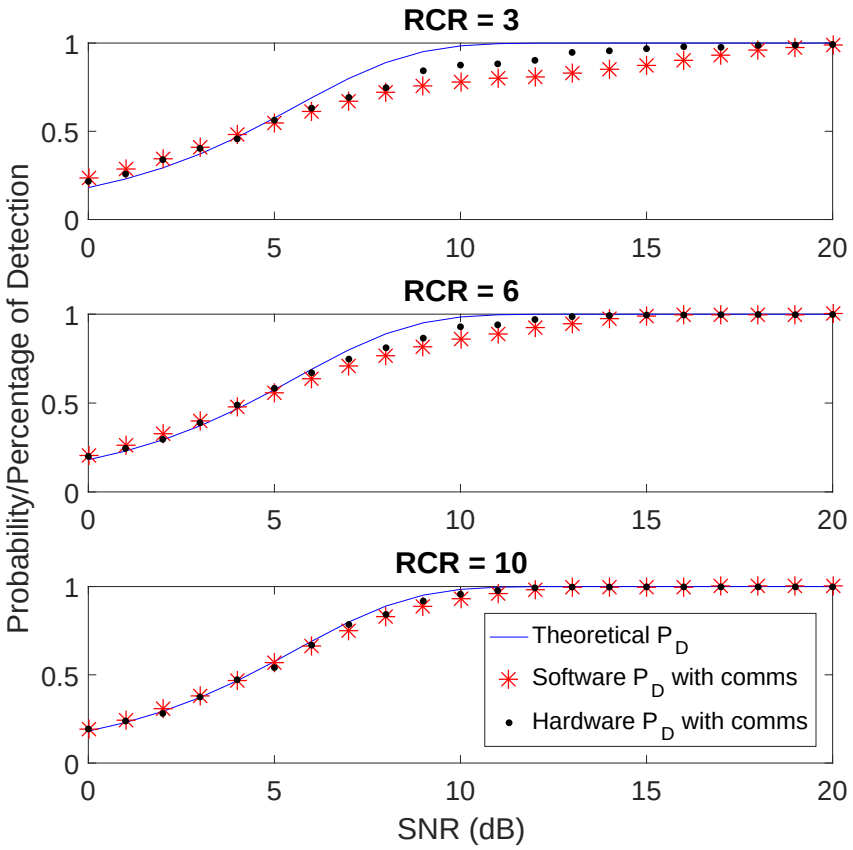

Figure 4.7. The Probability of Detection Results Compared for Theory, Software, and Hardware at Various RCR Values

the theoretical and software simulation results for the SRBR = 4.0 and SRBR = 32.0 cases. Additionally, these differences in the SRBR = 1.0 case likely come from the same reasons discussed above. Overall, hardware validation indicates that our software simulation is representative of the behavior of the radar architecture, and we expect similar results if this system were implemented on a real radar. As in the software simulation, the hardware detection probability results indicate that the addition of embedded intrapulse communications has little effect on the probability of detection of the radar. We now consider the effect of embedded intrapulse communications on range-Doppler maps (RDM) constructed from pulse Doppler radar.

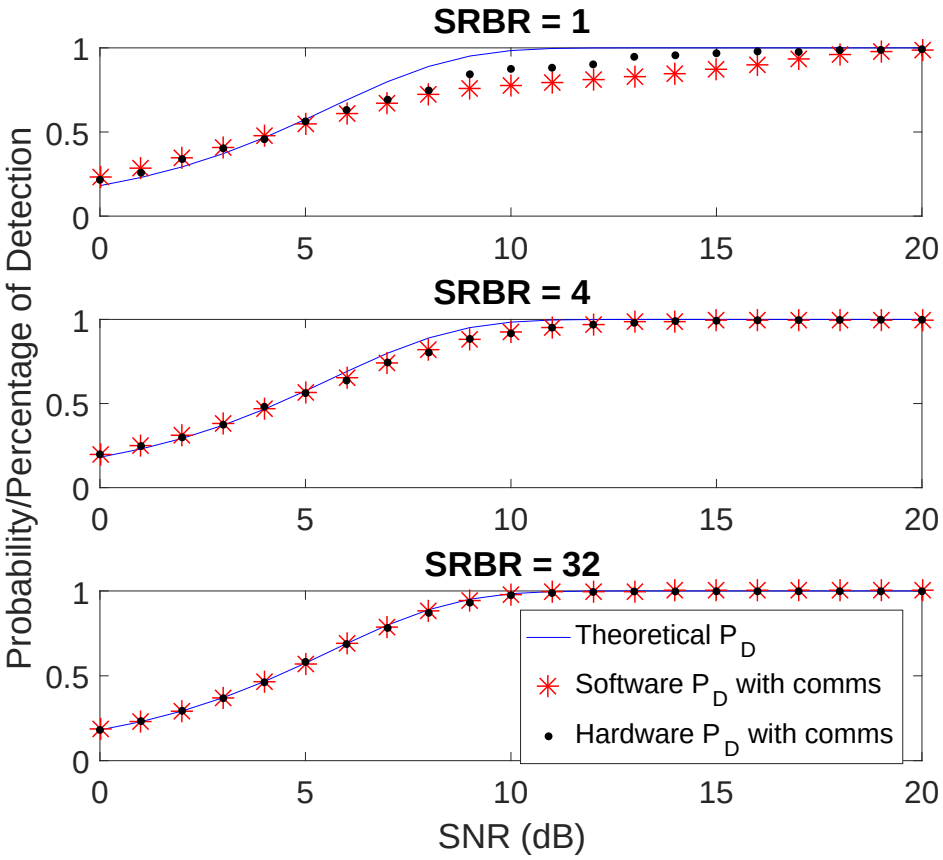

Figure 4.8. The Probability of Detection Results Compared for Theory, Software, and Hardware at Various SRBR Values

THIS PAGE INTENTIONALLY LEFT BLANK

CHAPTER 5:
Range-Doppler Maps

Pulse Doppler radar can be used to provide velocity information as well as range information for a detected target. One way to output this information so that it can be visualized is called a range-Doppler map (RDM). In this chapter, we investigate the effect of embedded intrapulse communications on the RDMs that are generated from pulse Doppler radar.

5.1 Theory

Pulse Doppler radar is based on the Doppler frequency shift, defined as

$$f_D = f_R - f_T, \tag{5.1}$$

where f_D is the Doppler frequency and f_R and f_T are the received and transmitted frequencies, respectively [8]. This Doppler frequency is related to the velocity of the target by

$$f_D = -\frac{2v}{\lambda_T}, \tag{5.2}$$

where v is the velocity of the target and λ_T is the wavelength of the transmitted signal [8]. Determining the Doppler frequency allows us to determine the velocity of the target. In order to determine the received frequency and, thus, the Doppler frequency, we assume a coherent pulse train of radar pulses that has already been downconverted to baseband, matched filtered, and sampled at intervals of the pulse repetition period [8]. We now have a number of I/Q samples equal to the number of radar pulses received at various delays. The delay time at which a radar pulse is received corresponds to the distance the target is from the radar. A diagram of the received signals is shown in Figure 5.1. In this diagram, the incoming pulses are sampled and stacked to obtain the I/Q time-domain received pulses. Then, a discrete Fourier transform implemented using the FFT algorithm is taken over the delay time in order to determine the Doppler frequency and thus the velocity of the target. The result of this FFT operation is the range-Doppler map, which contains range and Doppler bins corresponding to the target's distance and velocity. In the absence of noise, peaks in the RDM indicate the range and velocity of the targets [8]. In practice, when

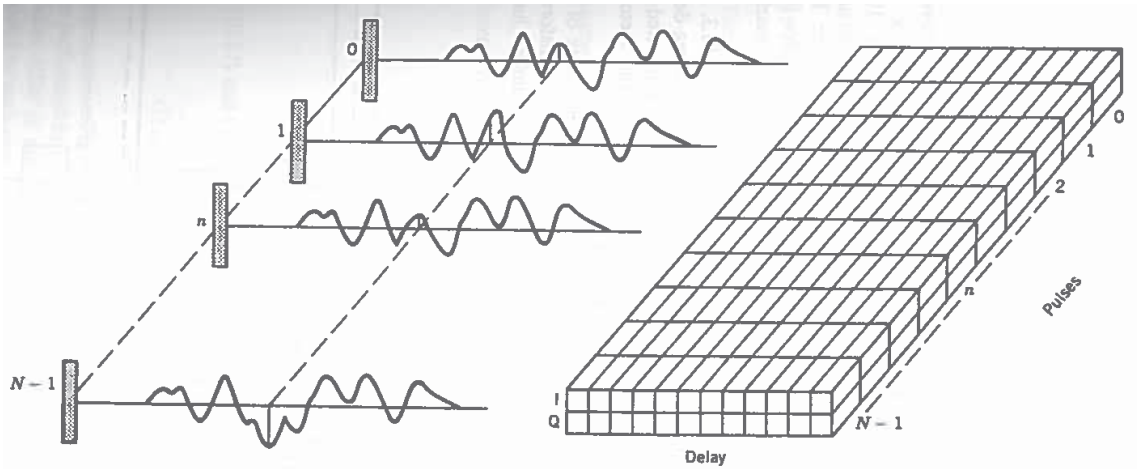

Figure 5.1. A Visualization of the Way Received Radar Pulses Are Stacked in the Creation of an RDM. Source: [8].

noise is present, we may not know exactly how many targets are present in the environment; however, as in Chapter 4, we can use a threshold (given some P_{FA}) to distinguish between a return from a target and noise. Of course, if we have a priori knowledge of the number of targets present, we can simply take that number of targets N_T and consider the N_T largest peaks in the RDM to be representative of the targets present. For the following situation, we assume there is one target in the RDM; therefore, the peak of the RDM is used to determine the range and velocity of the target present. A typical RDM for a radar signal with no embedded communications and one target is shown in Figure 5.2. In this figure, the same

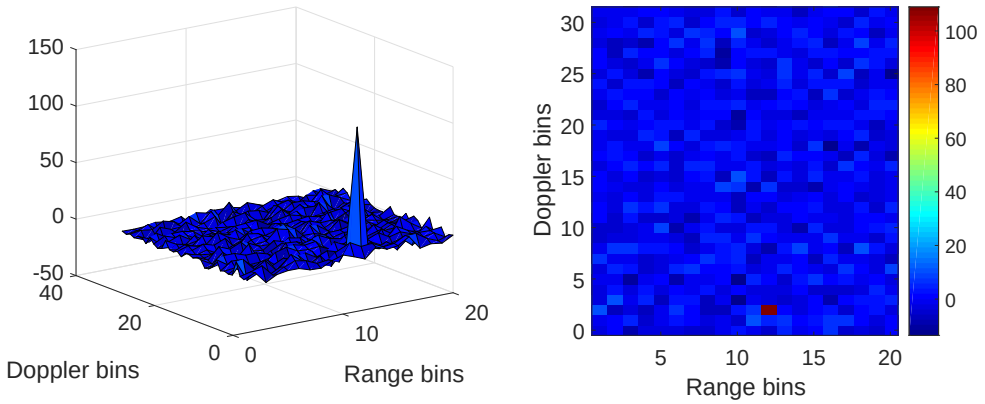

Figure 5.2. A Sample RDM with No Embedded Communications

information is displayed as both a three-dimensional graph (left) and a colormap (right). In

each case, the peak unambiguously occurs at a range bin of 12 and a frequency bin of three, as expected from the simulation code used to generate the plot. This RDM was generated using $N = 32$ coherent pulses which yield 32 possible Doppler bins. Additionally, there are 20 samples in each pulse-repetition interval, which yields 20 possible range bins. The SNR is 10 dB at the input of the receiver. After processing the pulse train, integration gain from the N pulses results in an output SNR of N times the input SNR, and so in this case, the output SNR is equal to 25 dB. Although there is no communications signal present for this RDM, the processing gain has the same multiplying effect on RCR as it does on SNR.

We now investigate the effects of the addition of embedded communications into the coherent radar pulses from which the RDM is constructed. Since each pulse is only sampled once, we do not vary the SRBR, as doing so makes no difference; therefore, we only vary the RCR.

5.2 Software Simulation

We again use MATLAB to perform the software simulation. As before, the matched filter in the radar receiver is matched to the communications-free radar pulse, but the radar return pulses contain embedded communications. Again, instead of setting a threshold that must be crossed to determine the presence of a target, we assume exactly one target is present. In the first scenario, we consider realistic signal parameters, which we define to be an input SNR of 10 dB and an input RCR of 10 dB for this case. The RDM from these parameters is shown in Figure 5.3. As shown in Figure 5.3, there is little discernable difference between the case with realistic signal parameters and the case with no communications. The peak value is still clearly visible and there is one largest value with all other values being much smaller.

We now deliberately select unrealistic signal parameters to illustrate the worst-case effect of embedded communications on an RDM. For this scenario, we choose the SNR to be 7 dB and the RCR to be -10 dB. The RDM from these signal parameters is shown in Figure 5.4. Even when the communications signal power is ten times the radar signal power, if we assume that the point with the largest magnitude contains a target, the correct range bin is still identified; however, while the correct Doppler bin is identified as the maximum value, there are now other values that are close to this maximum. As a result, the addition of

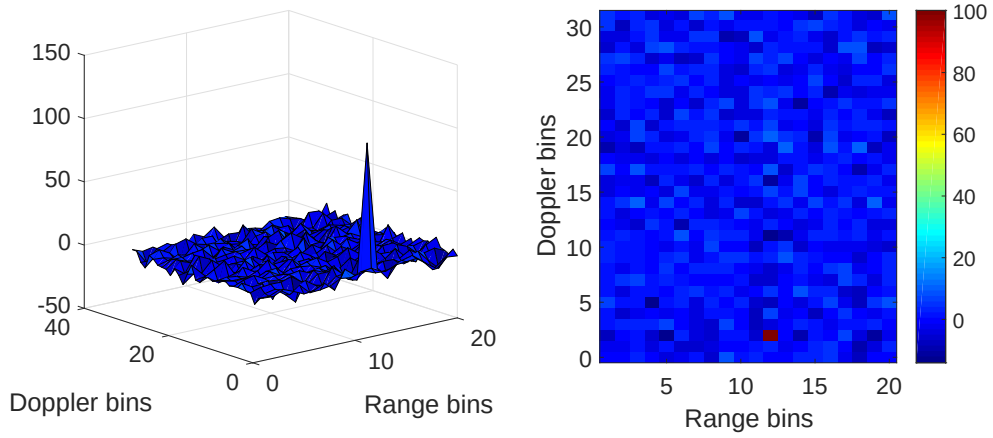

Figure 5.3. A Sample RDM with Realistic Signal Parameters

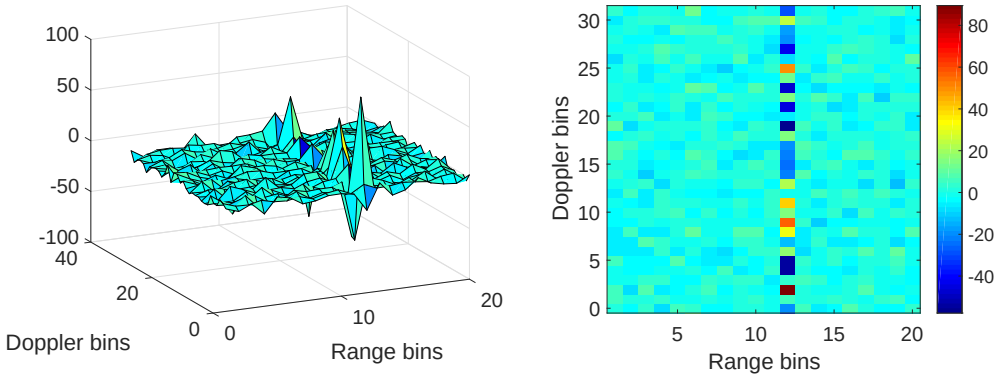

Figure 5.4. A Sample RDM with Unrealistic Signal Parameters

extremely high-powered communications interference can result in false velocity decisions if the assumption of one target is not maintained, as it could be incorrectly concluded that multiple targets are present at the same range but traveling at different velocities. This scenario is unlikely to occur due to the high-powered communications signal, which can no longer be considered LPI-like in the sense of this thesis, and so such an extreme result can be instead considered illustrative of the robustness of RDMs against interference from embedded intrapulse communications.

CHAPTER 6:
Navigational Perspective

We now consider the perspective of a radar user in a maritime environment. While in some sense this may be viewed as a continuation of the earlier chapter on probability of detection, in this chapter we seek to not merely understand the overall statistical performance of the radar with embedded intrapulse communications but rather to evaluate specific instances that are likely to occur in a maritime environment as well as the effect of radar-embedded communications on safe navigation.

6.1 Theory

Probability of detection, discussed in Chapter 4, assesses the statistical probability of a radar accurately identifying a target given a particular SNR and probability of false alarm P_{FA}. We are interested not merely in the overall effects of embedded intrapulse communications on radar probability of detection over many trials but also on the appearance of a navigational radar display when the radar return signal contains embedded communications. A sample radar display is shown in Figure 6.1. In this figure, a sample radar display on the left is

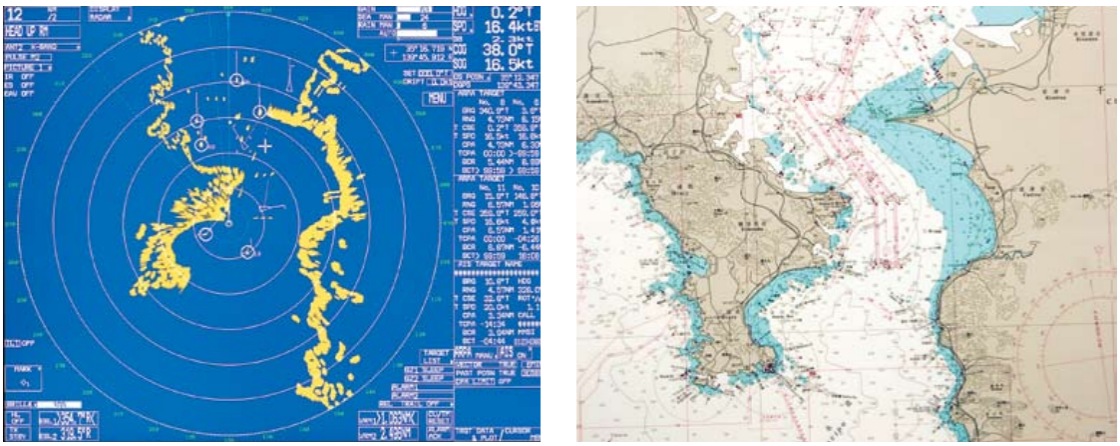

Figure 6.1. A Sample Radar Display. Source: [1].

compared to a chart of the area on the right. The contours of the coastline are clearly visible in the radar display, as well as several smaller returns that indicate other vessels. The vessel

on which the radar is mounted is located at the center of the radar display. While P_D is a statistical measure that indicates the frequency with which a target is detected by the radar, the figure shows the results of that target detection not over many trials but during usage in an actual maritime environment.

While the number of trials for probability of detection is much lower in the real-time maritime environment than in the Monte Carlo simulation used to simulate probability of detection, we still use $N > 1$ to simulate the averaging used by most modern radar displays to filter out noise [1].

6.2 Software Simulation

In order to simulate the navigational perspective, we again use MATLAB to simulate a navigation radar's rotational scanning capability.

6.2.1 Method

In order to imitate the radar's averaging noise-cancellation technique, we use $N = 5$ number of scans. Then, the radar return for a particular location is only plotted if it appears in at least four of the five scans. This averaging is adjustable by the radar user, but we fix these values for our simulations. Additionally, we use a P_{FA} of 0.01. The simulated target configuration used is shown in Figure 6.2. For this scenario, four targets are located within

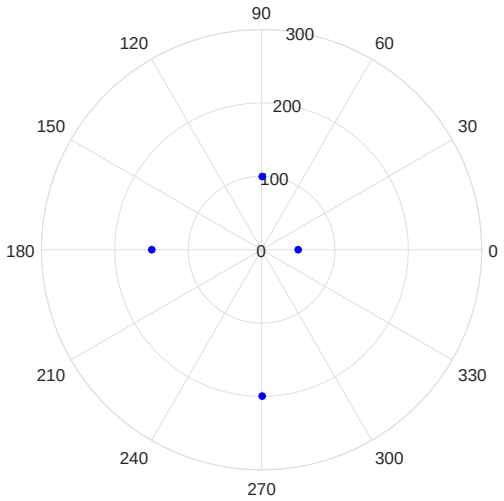

Figure 6.2. The Target Placement for Navigational Display Simulation

range of the radar, spaced over a range of angles and distances. Then, the matched-filtered received signal is compared to γ' to determine whether a target is present for each angle and distance value, using only noise if a target is not present at that point and noise along with the radar pulse with embedded communications if a target is present at that point. Two scenarios are proposed. The first scenario uses realistic signal parameters, with an SNR of 20 dB, an RCR of 10 dB, and an SRBR of 32. The second scenario uses intentionally unrealistic parameters as a worst-case scenario, with an SNR of 20 dB, an RCR of 0 dB, and an SRBR of 1.0.

6.2.2 Results

The results for the first scenario are shown in Figure 6.3, with the blue circle denoting a target location and the red square denoting a point that was identified as containing a target. As shown in the figure, using embedded intrapulse communications with realistic

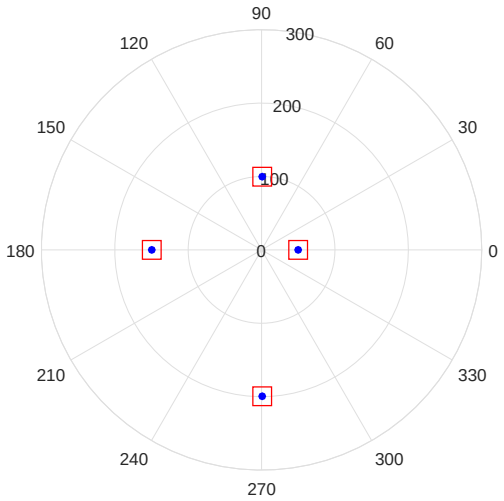

Figure 6.3. The Results for the Navigational Radar with Realistic Signal Parameters

signal parameters do not appear to affect the radar's performance, as all of the targets are correctly detected by the radar. In order to better understand at what point the embedded communications might affect the radar's ability to detect a target in a navigational environment, we use the intentionally unrealistic signal parameters described above. The results for this set of unrealistic parameters are shown in Figure 6.4. As shown in this figure, the presence of embedded communications causes the radar receiver to fail to detect two of the

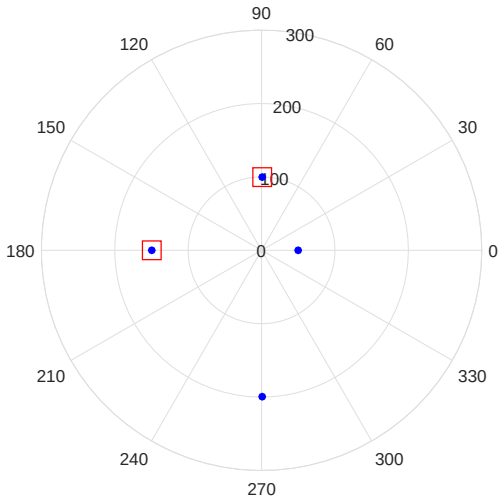

Figure 6.4. The Results for the Navigational Radar with Unrealistic Signal Parameters

four targets present. This is expected, as an RCR of 0 dB and an SRBR of 1.0 means that the communications signal has the same shape and magnitude as the radar pulse; therefore, when the communications signal is out of phase with the radar signal, the radar pulse is essentially cancelled out. This condition is a severe example of interference and not a relatively low-power signal interfering with a relatively high-power signal as described in the problem statement. This situation is therefore not a concern due to its inapplicability.

CHAPTER 7:
Conclusions and Recommendations

In this final chapter, we present overall conclusions drawing from the work of the previous chapters. Additionally, recommendations for future work arising from the outcome of this thesis research are presented.

7.1 Conclusions

Overall, the LPI-like nature of intrapulse embedded communications was verified. Additionally, the addition of intrapulse communications with sufficiently large RCR and SRBR does not appear to have a major effect on radar performance. Specifically, the PSD of radar signals with embedded communications was found to deviate negligibly from the PSD of the radar signal alone, so the presence of communications did not have a large effect on the radar signal in the frequency domain. Additionally, probability of detection for the combined radar and communications signal closely approximates the probability of detection for the radar signal alone as long as the SRBR value is at least 4 QPSK symbols per radar pulse. The addition of embedded communications was found to have negligible impact on range and velocity resolution for range Doppler maps where only one target is considered. Finally, the presence of embedded intrapulse communications does not appear to have a major negative effect on safe navigation. These results are encouraging and indicate that this area is worthy of future study and research.

7.2 Recommendations

The next step is to implement an embedded intrapulse communications system in hardware using the Furuno radar at NPS. While simulation provided an estimate of the effects of embedded intrapulse communications on pulsed radar, building this system in hardware will allow for measurements to be taken to determine whether or not an embedded communications system is a feasible method of communication, both in the inadvertent co-channel interference and intentional embedded communications cases.

Additionally, all simulation was performed for this thesis using the assumption that the radar

receiver used a matched filter architecture; however, some radars do not pass the received signal through a matched filter before determining whether an incoming signal is a radar return or not, using energy detection instead. Additional simulations could validate radar performance in the absence of a matched filter.

Finally, a simplifying assumption for this work was using a rectangular pulse shape for both the radar pulse and the QPSK symbols. Repeating the analyses performed here with pulse shaping for the radar and a band-limited pulse shape for the QPSK symbols, such as a raised-cosine pulse, would provide results relevant to pulse shaping.

List of References

[1] Operator's Guide to Marine Radar. Furuno. [Online]. Available: https://www.furunousa.com/Learning%20Center%20Documents/FurunoRadarGuide-LR.pdf. Accessed May 10, 2017.

[2] K. D. Shepherd and R. A. Romero, "Radar waveform design in active communications channel," in *Asilomar Conference on Signals, Systems and Computers*, Pacific Grove, CA, Nov. 2013, pp. 1515–1519.

[3] S. D. Blunt and C. R. Biggs, "Practical considerations for intra-pulse radar-embedded communications," in *International Waveform Diversity and Design Conference*, Kissimmee, FL, Feb. 2009, pp. 244–248.

[4] T. W. Tedesso, R. A. Romero, and Z. H. Staples, "Preliminary analysis of a covert communication method utilizing the presence of pulsed radar interference," in *IEEE International Conference on Acoustics, Speech, and Signal Processing*, New Orleans, LA, Mar. 2017.

[5] G. Meager, R. A. Romero, and Z. H. Staples, "Estimation and cancellation of high powered radar interference for communication signal collection," in *IEEE Radar Conference*, Philadelphia, PA, May 2016.

[6] T. T. Ha, *Theory and Design of Digital Communication Systems*. Cambridge, UK: Cambridge University Press, 2011, ch. 6.

[7] S. Miller and D. Childers, *Probability and Random Processes*. Waltham, MA: Academic Press, 2012, ch. 10.

[8] N. Levanon, *Radar Principles*. New York, NY: John Wiley & Sons, Inc., 1988.

[9] S. M. Kay, *Fundamentals of Statistical Signal Processing, Volume I: Estimation Theory*. Upper Saddle River, NJ: Prentice Hall, 1993.

THIS PAGE INTENTIONALLY LEFT BLANK

Initial Distribution List

1. Defense Technical Information Center
   Ft. Belvoir, Virginia

2. Dudley Knox Library
   Naval Postgraduate School
   Monterey, California